Ultraspecific and Highly Sensitive Nucleic Acid Detection by Integrating a DNA Catalytic Network with a Label-Free Microcavity

Yuqiang Wu,* David Yu Zhang,* Peng Yin, and Frank Vollmer*

Nucleic acid detection with label-free biosensors circumvents costly fluorophore functionalization steps associated with conventional assays by utilizing transducers of impressive ultimate detection limits. Despite this technological prowess, molecular recognition at a surface limits the biosensors' sensitivity, specificity, and reusability. It is therefore imperative to integrate novel molecular approaches with existing label-free transducers to overcome those limitations. Here, we demonstrate this concept by integrating a DNA strand displacement circuit with a micron-scale whispering gallery mode (WGM) microsphere biosensor. The integrated biosensor exhibits at least 25-fold improved nucleic acid sensitivity, and sets a new record for label-free microcavity biosensors by detecting 80 pM (32 fmol) of a 22nt oligomer; this improvement results from the catalytic behavior of the circuit. Furthermore, the integrated sensor exhibits extremely high specificity; single nucleotide variants yield 40- to 100-fold lower signal. Finally, the same physical sensor was demonstrated to alternatingly detect 2 different nucleic acid sequences through 5 cycles of detection, showcasing both its reusability and its versatility.

Dr. Y. Wu, Dr. F. Vollmer
Laboratory of Nanophotonics and Biosensing
Max Planck Insitute for the Science of Light
Erlangen 91058, Germany
E-mail: yuqiang.wu@mpl.mpg.de;
frank.vollmer@mpl.mpg.de

Dr. F. Vollmer
Division of Biomedical Engineering
Brigham and Women's Hospital
Harvard Medical School
Boston, USA

Dr. D. Y. Zhang
Department of Bioengineering
Rice University
Houston, USA
E-mail: dyz1@rice.edu

Dr. P. Yin
The Wyss Institute for Biologically Inspired Engineering
and Department of Systems Biology
Harvard Medical School
Boston, USA

1. Introduction

Because nucleic acids act to encode and regulate the expression of genes, sequence-specific detection of DNA and RNA is an important research and clinical goal.[1,2] Conventional diagnostic technologies often use fluorescence-based assays to localize and quantitate nucleic acid molecules of interest, driving much of molecular biology.[3,4] However, functionalizing oligonucleotides with fluorescent labels is typically a complex and expensive process that often skews physical and chemical properties, in turn affecting quantitative readout.[5]

Label-free technologies for detecting the concentration of nucleic acids, such as those based on plasmon resonance,[6,7] electrochemical conductance,[2,8] nanowires,[9] mechanical resonance,[10] micro-cantilevers,[11] or optical whispering gallery mode (WGM) resonance,[12–17] circumvent the need for fluorescence modifications; see **Table 1** for a comparison. In particular, optical WGM biosensors are emerging as one of the most versatile and sensitive label-free biosensing technologies, providing various mechanisms for sensing, sizing, trapping, and manipulation.[12–22] Although techniques based

Table 1. Comparison of label-free technologies for detecting the concentration of nucleic acids and for resolving single nucleotide polymorphism (SNP).

Label-free biosensor	Transducing mechanism	Microfluidic integration of arrays	Sensor reusable for different targets	DNA recognition mechanism (oligomer sensitivity)	Sensitivity and specificity in SNP detection
Plasmon resonance[6,7]	plasmon resonance shift[6,7,29]	yes[6]	no	direct hybridization (~0.1 nM)[2,30,31]	limited by kinetics and thermodynamics of direct hybridization at stringent conditions[23]
Electrochemical conductance[2,8]	conductance change[2,8]	large sensor arrays present a challenge[8]	no	direct hybridization (‹pM)[2,8]	enhanced by electrocatalysis in non-stringent conditions[2,8]
Nanowires[9,32]	conductance change, field effect[9,32]	yes[9]	no	PNA-DNA hybridization[32] (~fM)	high specificity requires PNA[32]
Nanomechanical resonator[10,11]	mechanical resonance frequency shift[10]	possible[33]	no	not demonstrated	not demonstrated
Microcantilever[11,34]	(optical) readout of cantilever bending[11]	yes[34]	no	direct hybridization[34] (~0.5 nM)	limited by direct hybridization[23]
WGM biosensor[12,13]	optical resonance red shift[16]	yes[22,24]	no	direct hybridization (~nM, for 22-mer)[22,24]	limited by direct hybridization[25]
WGM strand displacement sensor (this work)	optical resonance blue shift, transducer signal decoupled from analyte molecule	possible	yes	strand displacement (<80 pM / ~32 fmol, for 22-mer)	ultraspecific due to strand displacement circuit, robust to non-stringent conditions

on nanowire and electrochemical transducers have achieved very high sensitivity for detecting DNA and RNA concentrations, WGM biosensors are simple to fabricate, can be easily functionalized as well as multiplexed, and are made from inexpensive optical fibers.[13,15,17,21,22]

Sequence-specific detection by direct DNA hybridization on WGM devices faces three important challenges:[2,13,22–26] limited sensitivity, specificity, and reusability. First, years of work on advancing the device physics and engineering of WGM biosensors has improved the ultimate physical detection limits of WGM transducers.[12,16,19–21,27] Although WGM biosensors have shown great sensitivity for protein detection, the specific detection of DNA has been limited to 1 nanomolar concentrations due to specificity and sensitivity limits set by hybridization.[22,24–26,28] Novel molecular approaches are thus needed to overcome those limitations, mostly set by the inherent kinetics and thermodynamics of the process of molecular recognition through direct hybridization at the sensor surface. Second, non-cognate sequences that differ slightly in sequence may bind nonspecifically to the functionalized device, generating false positive signals and preventing proper detection. Finally, different sensors must be constructed to detect different nucleic acid sequences.

DNA strand displacement techniques have recently emerged as a novel family of approaches to enzyme-free homogenous detection assays.[35–38] Strand displacement circuits, for example, have been demonstrated to implement nucleic acid "catalysis" in which a nucleic acid sequence of interest effects the release of up to 100 nucleic acid molecules from metastable precursors; cascading such catalytic systems[38] has shown overall turnover of about 1000. Recently, strand displacement has been engineered to allow ultraspecific hybridization assays with specificity approaching the theoretical limit based on thermodynamics.[35] Although strand

displacement technologies have significantly improved the specificity and sensitivity of homogeneous detection assays, the readout for this technology has previously been constrained to gel electrophoresis or fluorescence readout, neither of which is easily applicable to point-of-care or clinical diagnostics.[35,38–40]

Here we combine the advantages of WGM label-free readouts and DNA strand displacement circuits by constructing an integrated label-free biosensor. Our work features the capabilities of DNA nanotechnology combined with highly sensitive optical microcavities for breaking through previous performance limitations in nucleic acid detection. This integrated biosensor exhibits at least 25-fold improvement in molecular sensitivity over the conventional hybridization-based WGM nucleic acid sensor. The integrated biosensor is highly specific, able to distinguish single nucleotide polymorphisms (SNPs) via kinetics of mass loading/unloading by a factor of 40 to 100. Finally, we demonstrate sequential detection of two different targets through five cycles of repeated use of the same WGM sensor device by isothermal exchange of buffer solutions.

2. System Design

2.1. WGM Biosensor

WGM biosensors are micron scale optical cavities, such as glass microspheres, capable of confining light by total internal reflection in a small modal volume and only at specific resonance wavelengths. These tiny optical resonators exhibit ultra-narrow linewidth, associated with very high quality Q factor, and are extremely sensitive to the binding
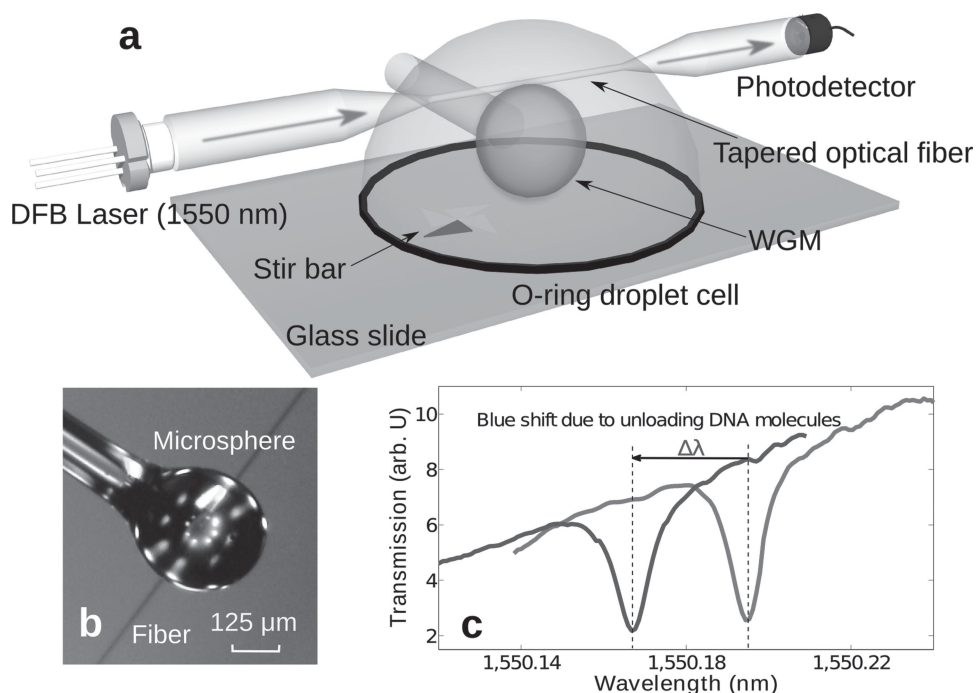
Figure 1. Experimental setup for WGM biosensor. (a) Light from a DFB laser (1550 nm) is coupled into and out of a WGM microsphere resonator through a tapered optical fiber. The droplet sample cell is prepared from an o-ring glued on a glass slide. A miniature magnetic stir bar homogenizes the reaction. WGM transmission spectra are acquired by the photodiode in real time while rapidly sweeping the DFB laser wavelength by ~0.2 nm. (b) A micrograph of a glass microsphere (diameter ~ 300 μm) coupled to a tapered optical fiber. (c) A typical spectrum of the microsphere, here before (red) and after (blue) the unloading of DNA from the surface of the microsphere.

of biomolecules to the microcavity surface. The changes in permittivity upon binding of analyte result in a shift of resonance wavelength. The high Q factor enables the precise monitoring of small resonance wavelength shifts, a method known as the reactive biosensing principle, which is emerging as one of the most sensitive label-free microsystems biodetection mechanisms.[12]

Only a small number of components are needed for an experimental realization of a WGM biosensor (**Figure 1**a). In this implementation, a continuous-wave tunable distributed feedback (DFB) laser diode, operating in the telecom band at ~1550 nm wavelength, excites a high Q WGM optical resonance in a silica microsphere via a tapered optical fiber. The taper is fabricated from single mode SMF-28 fiber using a microtorch to heat and at the same time pull apart the fiber. The microsphere is fabricated by melting the tip of a short piece of optical fiber so that surface tension in the melted glass tip forms a 300–400 μm in diameter silica microsphere. The microsphere-on-a-stem is then mounted on a microstage for controlled coupling to the tapered fiber region (Figure 1b), and after coupling, the fiber-coupled microsphere is immersed in a ~400 μL o-ring droplet cell. For specific DNA detection, the microsphere is functionalized with biorecognition elements, here ~22mer DNA oligonucleotides. The resonance wavelength shift of the sensor (Figure 1c), for example upon DNA hybridization, is quantitated in grams of nucleic acid mass loading per millimeter-squared sensor area, pg mm^{-2}, according to refs.[41,42]

$$massloading = \frac{\Delta\lambda}{\lambda} \frac{\left(n_s^2 - n_m^2\right)R}{2n_m \cdot dn/dc} \qquad (1)$$

where $\Delta\lambda$ is the shift of resonance wavelength, λ is the nominal wavelength of the DFB laser, $n_s = 1.46$ and $n_m = 1.33$ are the refractive indices of microsphere and aqueous medium, respectively, R is the approximate radius of the microsphere as determined by microscopic imaging, and $dn/dc \approx 0.17 \times 10^{-9}$ (mm^3 pg^{-1}) is the approximate incremental refractive index change of a DNA solution.[24] For the DNA detection experiments presented in this work, single-stranded DNA oligonucleotide probes were attached via biotin-streptavidin linkers to a dextran hydrogel that was coated onto the silica microsphere by physisorption.[24] The hybridization or dissociation of oligonucleotides with partial or full complementarity to these probes induces a mass change which can be observed from resonance wavelength shift, see Figure 1c and Experimental Section.

2.2. Molecular amplification

To improve the sensitivity of the WGM device at the molecular level, a "catalytic" DNA circuit based on strand displacement is designed, in which each molecule of the detection target effects the release of multiple molecules from multistranded precursor complexes.[38,43] The two precursor molecules, F and SBP (**Figure 2**a), are designed based on the

Figure 2. The WGM biosensor integrated with the DNA catalytic network. (a) The designed catalytic pathway. In the absence of detection target C, precursors SBP and F are metastable and do not interact significantly with each other. Target C acts catalytically to enable the reaction between SBP and F, resulting in the release of S and B from P. Domains (displayed as numbers) represent continuous subsequences of nucleic acids that act as a unit in hybridization and dissociation; starred domains are complementary to non-starred domains. Sequences are shown in Table 2. (b) Catalysis causes mass unloading from the microsphere sensor surface. The P molecules are attached to the WGM microsphere via a biotin-streptavidin interaction; through the course of the catalytic reaction, S and B are unloaded from the surface. (b, inset) Schematic of DNA molecules attached to the sensor surface via biotin-streptavidin linkers (see Experimental Section).

Ultraspecific and Highly Sensitive Nucleic Acid Detection by Integrating a DNA Catalytic Network with a Label-Free Microcavity

small
NANO MICRO

sequence of the detection target C. In the absence of C, SBP is double-stranded everywhere it is complementary to F, so no significant reaction occurs, and the two species are metastable. C reacts with SBP to generate intermediate complex CBP and byproduct S, the former of which can react with F via a newly exposed 5* domain. At the end of a reaction cycle, P is released as a single-stranded product, and C is released to enable multiple turnover. Previous characterizations of similar catalysis systems[38,43] reported catalytic speedup of over 10^4 and maximum turnover of about 100. Polyacrylamide gel electrophoresis (PAGE) was used to verify that the specific sequences used for this integrated WGM system behave qualitatively similarly in bulk solution (see Figure S3).

To integrate the catalytic system with the WGM label-free sensor, product P is designed with a 3' biotin modification, such that the SBP complex is initially functionalized to the glass microsphere via biotin-streptavidin interaction (Figure 2b inset). In the presence of analyte C, the catalytic reaction proceeds and S and B are released from P and the surface of the microsphere; this manifests as a surface mass unloading that yields a blue-shift of the resonance wavelength (Figure 1c). The integrated system should exhibit improved sensitivity to analyte C, compared to a conventional hybridization assay, because each molecule of analyte C results in the release of multiple copies of S and B from the microsphere due to catalytic turnover.

3. Results

3.1. Sensitivity Enhancement

To experimentally characterize the sensitivity improvement afforded by the integration of the catalytic system, first the sensitivity of a standard hybridization-based WGM sensor for detecting a 22-mer oligonucleotide analyte C by direct hybridization to its complement C* is determined. For this, the WGM biosensor surface is modified with complement C* via biotin-streptavidin interactions (see Experimental Section). The microsphere sensor is immersed in the droplet cell filled with Tris-EDTA buffer for ~10 min to allow temperature equilibration. Subsequently, a baseline sensogram was measured for ~200 s before analyte C was injected at various concentrations ranging from 50 to 2 nM. The mass loading response for three independent measurements are shown in **Figure 3**a. With 50 nM of C, microsphere surface was saturated after ~20 minutes of reaction, whereas for lower concentrations, the hybridization reaction continued to occur past ~40 minutes.

In the ~40 minutes during which the mass loading was observed, the detection limit for C is approximately 2 nM. These results in terms of sensor response and timescales are consistent with previous DNA detection schemes using label-free WGM biosensors and direct hybridization[24,26,28,44] (see also Figure S9). Because the number of C* molecules functionalized to the surface of the microsphere is far fewer than the number of C molecules in solution (even at 2 nM C, there

is 10× excess of C; see Supporting Infomation), we infer that the hybridization reaction is kinetically limited, potentially by diffusion. Thus, in principle, significantly lower concentrations of C could be detected given enough reaction time – however, extended assay times are not conducive for many biomedical applications.

Next the sensitivity of the integrated system with a DNA catalytic network is determined where in the presence of analyte C, S and B are released from P and the surface of the microsphere; this manifests as a surface mass unloading that yields a blue-shift of the resonance wavelength. Figure 3b shows the experimental results in which C catalytically unloads molecules from the microsphere surface. The microsphere surface is initially loaded with pre-annealed SBP complex. At t = 200 s, 4 μL of strand F is injected to the 400 μL droplet sample cell to a final concentration of 400 nM. At t = 400 s, analyte C is injected at concentrations of 50 nM (red), 10 nM (blue) 2 nM (magenta), 400 pM (green) or 80 pM (orange). The control trace (black) shows the behavior of the system in the absence of C.

To compare sensitivity at low concentrations the absolute initial slope of the mass loading (unloading) is used for quantification, a method established in WGM biosensing[14,22,25] (Figure 3c). With the integrated system, 80 pM concentration of analyte C produces a mass unloading initial slope of -0.17 pg mm^{-2} s (already corrected for the baseline slope from control experiment without target of -0.031 pg mm^{-2} s). For the conventional WGM sensor based on direct hybridization, 2 nM concentration of analyte C produces a mass loading initial slope of 0.076 pg mm^{-2} s, also corrected for the initial slope of 0.025 pg mm^{-2} s for the control experiments. Consequently, we have experimentally shown reliable detection of ~80 pM for 22-mer oligonucleotides, corresponding to at least 25-fold sensitivity improvement over the conventional WGM biosensor based on direct hybridization. At 80 pM concentration, there is less than 32 fmol of the DNA analyte in the droplet cell, setting a new sensitivity record for label-free DNA microcavity biosensors.[12,22]

Note that the total mass loading for the direct hybridization of target C is ~1200 pg/mm^2 (Figure 3a), while the total mass unloading for the WGM catalytic network mechanism is ~3500 pg mm^{-2} (Figure 3b). This shows that the WGM signal is indeed proportional to the length of oligonucleotides: the loaded sequence C is 22 nt long, and the unloaded sequences S and B are 20 and 49 nt long, respectively. This also confirms that the WGM biosensor can be reproducibly modified with biotin-streptavidin linked oligonucleotides at surface concentrations of ~10^{13} strands cm^{-2}, consistent with previous observations for the dextran surface functionalization technique.[24]

To determine the turnover of this integrated system an alternative version of F that does not allow multiple turnover was designed. In these experiments (Figure S4), the kinetics of mass unloading is slowed significantly. From these measurements we infer that for 2 nM of analyte C, the averaged the turnover is ~ 10 after 40 min (Supporting Information).

We have also challenged our integrated sensor device with the task of detecting DNA oligonucleotides in a
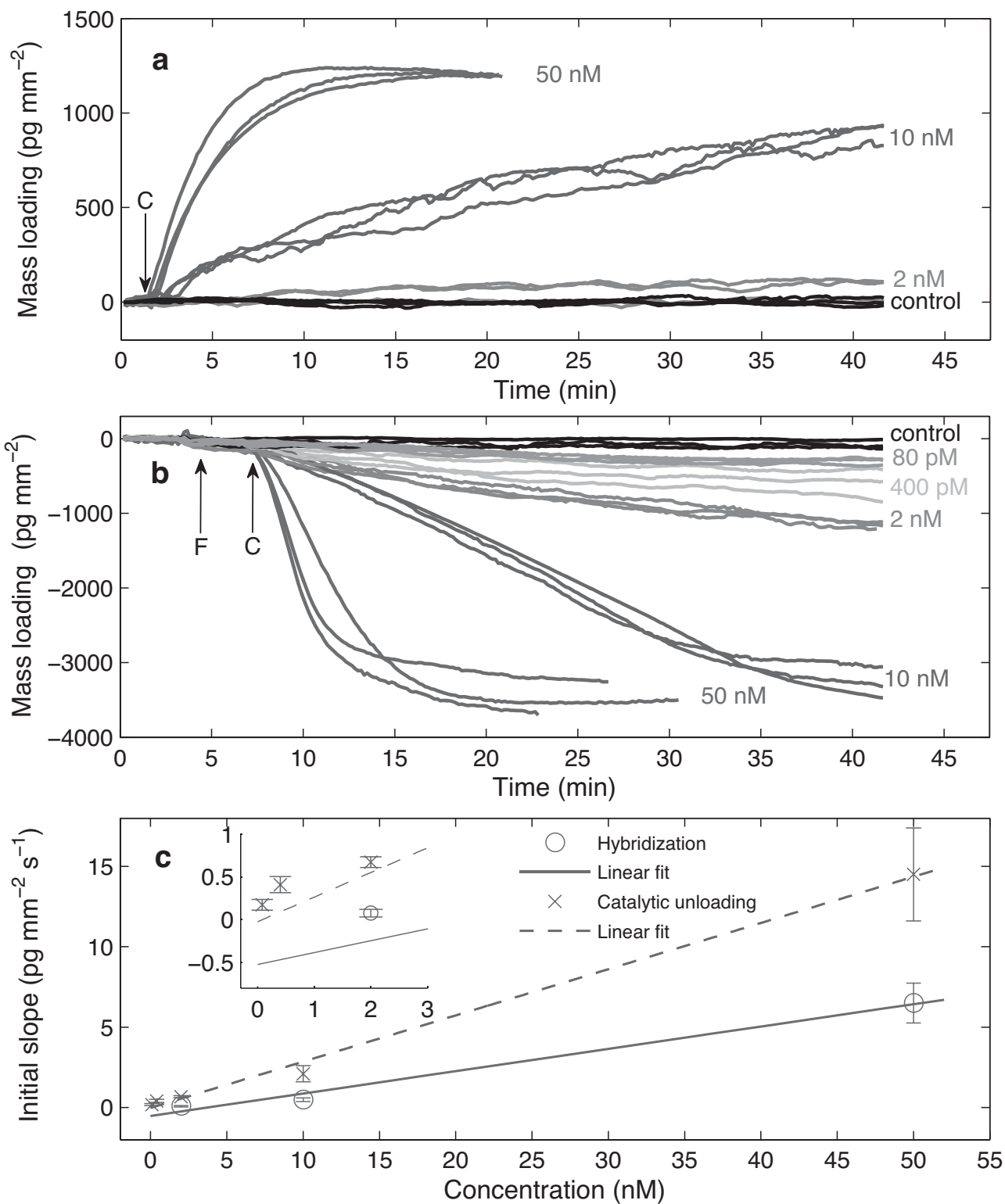
Figure 3. Comparison of molecular sensitivity of the conventional WGM sensor versus the integrated strand displacement biosensor. (a) Direct hybridization of target C onto the probe C* which was pre-attached to the microsphere surface. 4 µL of target sequence C was injected at t = 200 s into the sample cell with 400 µL buffer to achieve final C concentrations of 50 nM (red), 10 nM (blue) or 2 nM (magenta). Control experiments (black) were done by immersing the sensors in the sample cell without injecting anything. (b) Integrated biosensor in which target C catalytically unloads strands S and B. 4 µL of F was injected at t = 200 s into the sample cell with 400 µL buffer to achieve final F concentration of 400 nM. At t = 400 s, 4 µL of C was injected to achieve final concentrations of 50 nM (red), 10 nM (blue) 2 nM (magenta), 400 pM (green) or 80 pM (orange). The control trace (black) shows the behavior of the system in the absence of C. (c) Averaged absolute initial slopes of mass loading/unloading for direct hybridization (red circle) and catalytic unloading (blue cross) as a function of concentration. The solid/dashed lines are the linear fit. (c, inset) A close-up for low concentrations.

NANO MICRO

small

Ultraspecific and Highly Sensitive Nucleic Acid Detection by Integrating a DNA Catalytic Network with a Label-Free Microcavity

complex media for which we chose TE buffer with 10% fetal calf serum (FCS). Although the amplitude of our sensor response was reduced due to nonspecific bindings of FCS (Figure S5), our results show that our sensor is indeed able to detect target oligonucleotides with concentrations as low as 80 pM – even in a complex media (Figure S6).

3.2. Ultraspecificity and Single Nucleotide Discrimination

Typically, label-free sensors based on hybridization struggles with single base specificity and discrimination of closely related nucleic acid analytes, due to the thermodynamic favorability of hybridization of non-cognate analytes with highly similar sequences. Although specificity for any particular nucleic acid analyte/probe pair can be optimized by solution salinity and temperature,[25] this process is time consuming and imperfect, and not conducive to significant multiplexing. Similarly, the suppression of nonspecific interactions is essential to multiplexed detection.

Strand displacement circuits have overcome many of these challenges, and the integrated WGM sensor should in principle inherit the ultraspecificity properties of strand displacement systems. However, surface chemistry is known to deviate significantly from solution chemistry in both thermodynamics and kinetics, so it is necessary for us to experimentally test the integrated sensor's specificity.

To provide a benchmark for comparison, the standard hybridization-based WGM sensor was tested. We challenged this sensor with 3 single nucleotide variants of the intended analyte C (Cm5aG, Cm11cT, and Cm14gC; **Figure 4**a). The

three single base changes (A to G at position 5, C to T at position 11, G to C at position 14), were selected to be representative of the variety of both positions along the analyte sequence and of the thermodynamics of single-base changes. These single nucleotide variants induced a similar kinetics and total amount of mass loading as the analyte C, so the standard WGM sensor is **not** specific to SNPs.

Figure 4b shows the integrated strand displacement WGM sensor challenged by the same single nucleotide variants. Here, the single nucleotide variants showed significantly lower mass unloading than that of the intended analyte C. Quantitatively, a linear fit determined the initial slopes[22] of the unloading to be −14.5, −0.4, −0.13 and −0.1 pg mm^{-2} s for 50 nM C, Cm5aG, Cm11cT and Cm14gC respectively. From these unloading rates, we infer single-base specificity of the integrated biosensor to be between 40 (−14.5/−0.4) and 100 (−14.5/−0.1). The initial slight increase in mass loading may be due to the fact that the initial on-rates of the hybridization of some single nucleotide variants are higher than the unloading off-rates. This molecular specificity matches or exceeds the performance of strand displacement systems in bulk solution,[43] and represents the first experimental demonstration of nucleic acid ultraspecificity at a surface.

3.3. Versatility and Reusability

Typical label-free nucleic acid detection technologies based on hybridization suffer from the limitation that a different functionalized device is needed to detect each different sequence. Furthermore, each device can generally be only used once; dehybridizing oligonucleotides requires harsh buffer conditions, high temperature, or practically takes too long.[2,45] Here, the integrated sensor overcome both limitations: the same integrated WGM-strand displacement device can be reused to detect different sequences.

We first show that microspheres functionalized with the same DNA sequence (P) could be used for the versatile detection of different analytes (Figure S7). This is feasible for our integrated system because the sequence of P is independent of the sequence of the detection target C. To detect a different target C2 (based on the vertebrate specific mir-194), a different set of sequences F2, S2, and B2, was designed which enables the same P-functionalized microsphere to detect C2.

The integrated system, in detecting the second analyte C2, exhibits significantly slower mass unloading than in detecting C. DNA folding software[46] indicates that the F2 precursor possesses significant secondary structure. Thus, we believe that the kinetic slowdown is due to the kinetics of spontaneous unfolding of F2.[40] In this particular case, the sequence
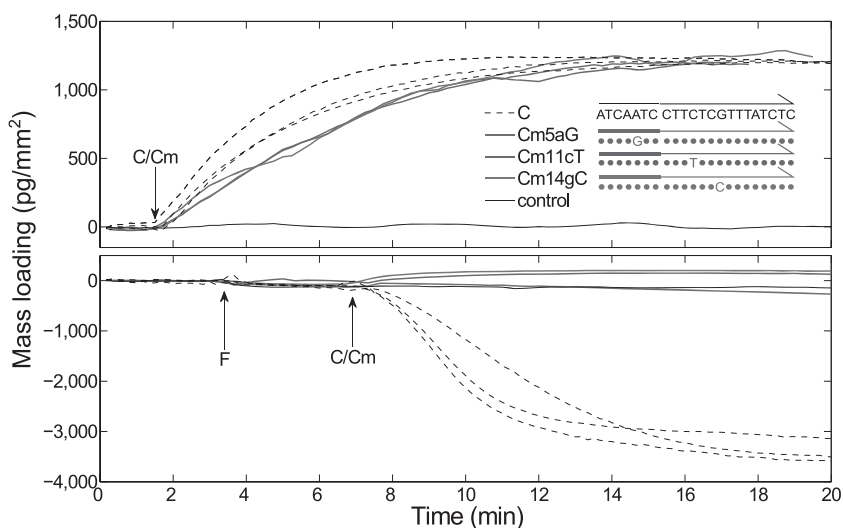
Figure 4. Comparison of single nucleotide polymorphism (SNP) specificity of the conventional WGM biosensor versus the integrated biosensor. (a) SNP detection with the conventional hybridization method. The target (dashed lines) and three single nucleotide variants (red, blue, and green) were injected at t = 100 sec at 50 nM concentration. The inset shows the sequences of the target and the single nucleotide variants; the thicker line segment denotes the toehold region. (b) SNP detection with the integrated biosensor. F with a final concentration of 400 nM was injected at t = 200 s and followed by the injection of target or single nucleotide variant (C and Cms, respectively) at t = 400 s to a concentration of 50 nM. Colors of traces are consistent with those shown in panel (a). The initial slight increase in mass loading due to single nucleotide variants may be due to nonspecific interactions and/ or physical perturbation of system due to addition of reagents.
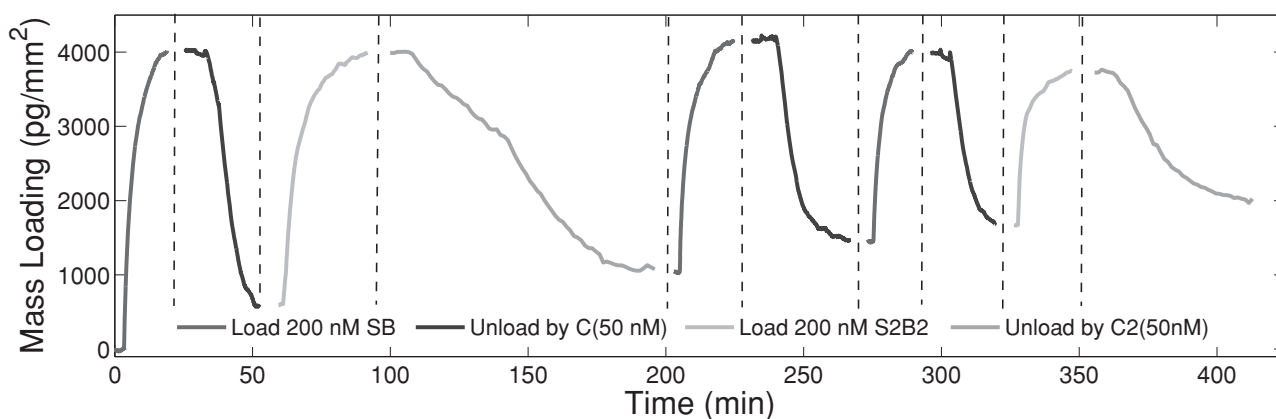
Figure 5. Repeated reuse of integrated WGM biosensor to detect multiple different target sequences. Loading experiments were performed with 200 nM of SB/S2B2 and unloading experiments were performed with 400 nM F/F2 and 50 nM C/C2. The mass loadings were converted from the relative shifts of each loading/unloading cycle and offset so that the next loading/unloading cycle starts where the last one ended.

of F2 is determined partially by the sequence of the common product P, and partially by the sequence of the analyte C2. The sequence of P, in turn, was designed specifically to avoid undesirable interactions with the first analyte C, and thus resulted in unintended secondary structure of F2. Careful sequence design of P that considers all analytes should be able to overcome the kinetic slowdown due to secondary structure observed here for C2. Nonetheless, even with this non-ideal sequence setup, C2 is still reliably detected by the WGM strand-displacement sensor.

Next, the same WGM microsphere is shown to be reusable. At the end of a detection reaction, the products S and FB and the analyte C are released from the microsphere surface; consequently, through a mild buffer exchange and the WGM biosensor can be restored to allow repeated detection cycles (Figure S8). There is gradual decrease of maximum sensor signal (approximately 13% per cycle) upon repeated reuse of the same WGM device. The degradation of the sensor surface occurs when the functionalized microsphere is taken out of the droplet cell and partially dried in air. This degradation due to partial drying can be avoided in future devices integrated with microfluidics which will allow all steps of the detection cycle to be performed in solution.

Finally, we combine these two properties and show that the same WGM microsphere (functionalized with the same P molecules) can be used through 5 distinct cycles of detection to alternatingly detect 2 different sequences. The concept is demonstrated in **Figure 5**.

4. Conclusion

For real-time, label-free nucleic acid detection, the integrated WGM biosensor provides three major advantages over conventional label-free biosensor approaches: molecular sensitivity, molecular specificity, and device reusability. Experimentally, we here showed at least 25-fold enhancement of the sensitivity and detection down to ~80 pM (32 fmol) of a 22-mer DNA oligo both in clean buffer and FCS, SNP discrimination by a factor of 40 to 100, and versatile detection

by the same physical microsphere of 2 different analytes over 5 cycles of use.

The high sensitivity of the catalytic WGM strand-displacement is attributed to both the fact that the target DNA can catalytically trigger many detection events, and the fact that the mass unloading is greater than the size of the analyte oligonucleotide. The current catalyst system exhibits a turnover of about 10 in the course of the 40 minutes of reaction observed. Previous[43] studies have shown that the catalytic turnover can be optimized to over 100 by adjustments such as the 5'/3' orientation of molecules, the types of post-synthesis purifications, and the sequence design of the molecules. Furthermore, cascading two or more stages of catalysis[38] allows asymptotically faster release kinetics and exponentially higher turnover. Additionally, because the mass of the analyte is decoupled from the mass being unloaded, the use of bulkier pre-loaded molecules (S and L for this manuscript) can provide another easy way of significantly improving sensitivity. Consequently, the achievements shown in this manuscript are but the tip of an iceberg; significantly more sensitivity label-free detection devices are on the horizon by further exploring the integration of strand displacement circuits with label-free biosensors.

The ultraspecificity displayed by the integrated WGM sensor is close to the theoretical maximum allowed by the thermodynamics of single base changes.[35] Discrimination against single nucleotide variants of the intended analyte is robust to position and base identity of the SNP. Previous work has shown that in solution, these ultraspecific strand displacement systems retain their properties across a wide range of temperatures and salinities; although these properties were not tested here, we likewise believe that the integrated WGM biosensor can be robustly specific regardless of environmental conditions.

The demonstrations of versatility and reusability of the integrated WGM biosensor are important proofs-of-concept for transitioning this technology from the laboratory to real-world diagnostic applications. By allowing the same type of DNA-functionalized glass microspheres to be generally used for the detection of any arbitrary nucleic acid biomarker,

device manufacturing costs are sharply reduced. By allowing the same physical microsphere device to be used across multiple cycles of operation, the number of devices needed by the end-users is reduced. Consequently, we are optimistic about the application of integrated WGM biosensors to point-of-care diagnostics.

5. Experimental Section

WGM biosensor setup: Silica microspherical WGM resonators with diameters ranging from 300 to 400 μm were fabricated by melting the tip of optical fibers (SMF-28) with an oxygen-butane microtorch. The WGMs are excited by evanescent coupling the microsphere to a tapered optical fiber made by the standard heat-and-pull technique. The wavelength of a tunable distributed feedback laser (DFB) operating ~1550 nm is scanned every millisecond to obtain a transmission spectrum of WGMs with a spectral width of ~0.2 nm. The spectra are recorded using LabVIEW program. The sample cell was prepared from an o-ring glued onto a glass slide. Inside our sample cell we place a miniature magnetic stir bar to homogenize the reactions. The schematic of the setup is shown in Figure 1a.

Microsphere surface modification: Microspheres were cleaned in an air oxygen plasma for 5 minutes immediately after fabrication, then immersed in a 2 μL hanging drop of a dextran-biotin solution (10 mg/ml, Life Technologies) until almost dry.[24] After a brief rinse in water for 5 min, they are then incubated until almost dry in a hanging drop of 2 μL of 8 μM solution of biotinylated DNA oligonucleotides (C* or P), coupled to streptavidin at a molar ratio of ~2:1. After incubation, spheres are rinsed again in the water and stored there until use. The dextran hydrogel coating is ideal for functionalizing the WGM biosensor since it prevents unspecific binding of DNA and supports a high surface density of attached biotin molecules that link to biotinlyated oligonucleotides via streptavidin. We have optimized the surface chemistry of dextran physisorption and repeatedly achieve a surface density of ~10^{13}/cm^2 for biotin-streptavidin-linked DNA oligonucleotides (see Figure S1 & S2).

DNA oligonucleotides and buffer conditions: The DNA oligonucleotides used in this study were purchased from Experience Eurofins MWG Operon. DNA oligonucleotides were purified by Eurofins using high-performance liquid chromatography (HPLC). Individual DNA oligonucleotides were re-suspended and stored in Tris-EDTA (TE) buffer (10 mM Tris-HCl pH balanced to 8.0, with 1 mM disodium EDTA, purchased from Sigma-Aldrich) at 4 °C. Directly preceding experiments, TE buffer is mixed with a final MgCl$_2$ concentration of 12.5 mM. Because ~1 mM of the Mg^{2+} is chelated by the EDTA present in solution, the free concentration of Mg^{2+} is estimated to be 11.5 mM. All DNA sequences are listed in **Table 2** and Table S1.Fetal calf serum was purchased from Biochrom, Merck Millipore.

Table 2. Sequences of the oligonucleotides.

Domain	Sequences	Length (nt)
C	5′-ATCAATC CTTCTCGTTTATCTC-3′	22
C*	5′-biotin-GAGATA AACGAGAAG GATTGAT-3′	22
S	5′-CTTCTCGTTTATCTCCTGTA-3′	20
B	5′-GCGATG GGTAAGAACTTTAGTG TACAG GAGATAAACGAGAAG GATTGAT-3′	49
F	5′-CTTCTCGTTTATCTC CTGTA CACTAAAGTTCTTACC-3′	36
P	5′-CACTAAAGTTCTTACC CATCG-biotin-3′	21
Cm5aG	5′-ATCAGTC CTTCTCGTTTATCTC-3′	22
Cm11cT	5′-ATCAATC CTTTTCGTTTATCTC-3′	22
Cm14gC	5′-ATCAATC CTTCTCCTTTATCTC-3′	22

[1] D. P. Bartel, *Cell* **2009**, *136*, 215.
[2] A. Sassolas, B. D. Leca-Bouvier, L. J. Blum, *Chem. Rev.* **2008**, *108*, 109.
[3] S. Tyagi, *Nat. Methods* **2009**, *6*, 331.
[4] G. Liti, D. M. Carter, A. M. Moses, J. Warringer, L. Parts, S. A. James, R. P. Davey, I. N. Roberts, A. Burt, V. Koufopanou, I. J. Tsai, C. M. Bergman, D. Bensasson, M. J. T. O/'Kelly, A. van Oudenaarden, D. B. H. Barton, E. Bailes, A. N. Nguyen, M. Jones, M. A. Quail, I. Goodhead, S. Sims, F. Smith, A. Blomberg, R. Durbin, E. J. Louis, *Nature* **2009**, *458*, 337.
[5] S. A. E. Marras, F. R. Kramer, S. Tyagi, *Nucleic Acids Res.* **2002**, *30*.
[6] J. N. Anker, W. P. Hall, O. Lyandres, N. C. Shah, J. Zhao, R. P. Van Duyne, *Nat. Mater.* **2008**, *7*, 442.
[7] J. Homola, *Chem. Rev.* **2008**, *108*, 462.
[8] T. G. Drummond, M. G. Hill, J. K. Barton, *Nat. Biotechnol.* **2003**, *21*, 1192–1199.
[9] F. Patolsky, G. Zheng, C. M. Lieber, *Nanomedicine* **2006**, *1*, 51–65.
[10] J. L. Arlett, E. B. Myers, M. L. Roukes, *Nat. Nanotechnol.* **2011**, *6*, 203.
[11] P. S. Waggoner, H. G. Craighead, *Lab Chip* **2007**, *7*, 1238.
[12] F. Vollmer, L. Yang, *Nanophotonics* **2012**, *1*, 267.
[13] X. D. Fan, I. M. White, S. I. Shopova, H. Y. Zhu, J. D. Suter, Y. Z. Sun, *Anal. Chim. Acta* **2008**, *620*, 8.
[14] A. Qavi, A. Washburn, J.-Y. Byeon, R. Bailey, *Anal. Bioanal. Chem.* **2009**, *394*, 121.

[15] H. K. Hunt, A. M. Armani, *Nanoscale* **2010**, *2*, 1544.
[16] F. Vollmer, S. Arnold, *Nat. Methods* **2008**, *5*, 591.
[17] T. Yoshie, L. Tang, S.-Y. Su, *Sensors* **2011**, *11*, 1972.
[18] S. Lin, K. B. Crozier, *Lab Chip* **2011**, *11*, 4047.
[19] T. Lu, H. Lee, T. Chen, S. Herchak, J. H. Kim, S. E. Fraser, R. C. Flagan, K. Vahala, *Proc. Natl. Acad. Sci. U.S.A.* **2011**, *108*, 5976.
[20] X. Lopez-Yglesias, J. M. Gamba, R. C. Flagan, *J. Appl. Phys.* **2012**, *111*, 84701.
[21] F. Vollmer, S. Arnold, D. Keng, *Proc. Natl. Acad. Sci.* **2008**, *105* , 20701.
[22] A. J. Qavi, R. C. Bailey, *Angew. Chemie-International Ed.* **2010**, *49*, 4608.
[23] K. Nakatani, *Chembiochem* **2004**, *5*, 1623.
[24] F. Vollmer, S. Arnold, D. Braun, I. Teraoka, A. Libchaber, *Biophys. J.* **2003**, *85*, 1974.
[25] A. J. Qavi, T. M. Mysz, R. C. Bailey, *Anal. Chem.* **2011**, *83*, 6827.
[26] J. D. Suter, I. M. White, H. Y. Zhu, H. D. Shi, C. W. Caldwell, X. D. Fan, *Biosens. Bioelectron.* **2008**, *23*, 1003.
[27] J. Zhu, S. K. Ozdemir, Y.-F. Xiao, L. Li, L. He, D.-R. Chen, L. Yang, *Nat Phot.* **2010**, *4*, 46.
[28] O. Scheler, J. T. Kindt, A. J. Qavi, L. Kaplinski, B. Glynn, T. Barry, A. Kurg, R. C. Bailey, *Biosens. Bioelectron.* **2012**, *36*, 56.
[29] K. A. Willets, R. P. Van Duyne, in *Annu. Rev. Phys. Chem., Annual Reviews, Palo Alto* **2007**, 267.
[30] E. Milkani, S. Morais, C. R. Lambert, W. G. McGimpsey, *Biosens. Bioelectron.* **2010**, *25*, 1217.
[31] H. Šípová, J. Homola, *Anal. Chim. Acta* **2013**, *773*, 9.

[32] J. Hahm, C. M. Lieber, *Nano Lett.* **2004**, *4*, 51.
[33] T. P. Burg, M. Godin, S. M. Knudsen, W. Shen, G. Carlson, J. S. Foster, K. Babcock, S. R. Manalis, *Nature* **2007**, *446*, 1066.
[34] F. Huber, H. P. Lang, N. Backmann, D. Rimoldi, C. Gerber, *Nat. Nanotechnol.* **2013**, *8*, 125.
[35] D. Y. Zhang, S. X. Chen, P. Yin, *Nat. Chem.* **2012**, *4*, 208.
[36] P. Yin, H. M. T. Choi, C. R. Calvert, N. A. Pierce, *Nature* **2008**, *451*, 318.
[37] B. L. Li, A. D. Ellington, X. Chen, *Nucleic Acids Res.* **2011**, *39*, e110.
[38] D. Y. Zhang, A. J. Turberfield, B. Yurke, E. Winfree, *Science* **2007**, *318*, 1121.
[39] D. Y. Zhang, G. Seelig, *Nat. Chem.* **2011**, *3*, 103.
[40] D. Y. Zhang, E. Winfree, *J. Am. Chem. Soc.* **2009**, *131*, 17303.
[41] M. Baaske, F. Vollmer, *ChemPhysChem* **2012**, *13*, 427.
[42] S. Arnold, M. Khoshsima, I. Teraoka, S. Holler, F. Vollmer, *Opt. Lett.* **2003**, *28*, 272.
[43] D. Y. Zhang, E. Winfree, *Nucleic Acids Res.* **2010**, *38*, 4182.
[44] J. D. Suter, D. J. Howard, H. Shi, C. W. Caldwell, X. Fan, *Biosens. Bioelectron.* **2010**, *26*, 1016.
[45] M. Lee, D. R. Walt, *Anal. Biochem.* **2000**, *282*, 142.
[46] M. Zuker, *Nucleic Acids Res.* **2003**, *31*, 3406.